Patient-Specific Finite Element Models of Transtibial Amputation in Several Prosthetic Users: The Inter-Subject Variability

S. Portnoy[1], I. Siev-Ner[2], N. Shabshin3, A. Kristal[2], Z. Yizhar[4], A. Gefen[1]

[1]Department of Biomedical Engineering, Tel Aviv University, Ramat Aviv, Israel
[2]Department of Orthopaedic Rehabilitation, Chaim Sheba Medical Center, Israel
[3]Department of Diagnostic Imaging, Chaim Sheba Medical Center, Israel
[4]Department of Physical Therapy, Tel Aviv University, Ramat Aviv, Israel

Abstract— **Active transtibial amputation (TTA) patients are at risk for developing pressure ulcers and deep tissue injury (DTI) while using their prosthesis. It is therefore important to obtain knowledge of the mechanical state in the internal soft tissues of the residuum, as well as the mechanical state upon its surface. For this purpose we employed patient-specific MRI-based non-linear 3D finite element models to quantify the internal mechanical conditions in 3 residual limbs of TTA prosthetic users during load-bearing. The geometrical characteristics of the residuum of the TTA participants varied significantly between patients, e.g. the residuum lengths were 7.6, 9.2 and 13.3cm. We generally found that internal strains were higher in the bone proximity than in the muscle periphery. The highest strains were found in the 7.6cm-long residuum. Correspondingly, the lowest strains were found in the 13.3cm-long residuum, which had the thickest muscle flap. Yet even in the case of a long residuum, a third of the distal tibial proximity area was occupied by internal principal compression strains above 5%. For both patients with shorter residual limbs, the internal principal compression strains above 5% occupied almost the entire distal tibial proximity area. We conclude that the wide viability between residual limbs necessitate quantitative analysis of internal mechanical state in the TTA individual to assess the risk for DTI onset.**

Keywords— **Deep tissue injury, finite element modeling, pressure ulcer, rehabilitation**

I. Introduction

Deep tissue injury (DTI) is a life-threatening complication that initiates in a muscular tissue underlying a bony edge [1]. This injury is most common in wheelchair bound patients but also occurs in bed-ridden patients and lower limb amputees while using their prostheses. Transtibial amputation (TTA) dictates a new loading state in the severed limb via the posterior calf muscles, now folded under the truncated bones. The gastrocnemius muscle flap and fat tissue cushioning the truncated tibia and fibula may precariously undergo large deformation and ischemia during load bearing, which may leads to cell death in the internal soft tissues. Even at a critical state of tissue necrosis, visual detection of the DTI on the skin of the patient will frequently result in a wrongful diagnosis as a pressure ulcer (PU) type I, i.e. superficial skin-deep wound. Most TTA occur due to vascular diseases, which are sometimes coupled with a certain level of peripheral neuro-deficiency. The TTA residuum inside the prosthetic socket is therefore endangered by the lack of sensorial alert to the formation of DTI. While laboring to avoid hazardous falls and maintain stability and symmetrical gait during daily activities, an internal ulcer may spread to surrounding tissues, inevitably resulting in hospitalization of the patient and possibly death.

Previous researches quantified surface skin-prosthetic socket stresses and temperatures using various sensors and computational modeling of the residuum as a first step in achieving socket optimization. These studies utilized interface stresses to evaluate socket alignment, different foot components, socks, liners and so on, while disregarding the internal mechanical condition of the residuum. Unfortunately, there is little correlation between interface stresses in the TTA socket and internal stresses in the bone proximity, where DTI initiates. Depending on the unique geometry of the individual TTA residuum, we hypothesize that the mechanical condition of internal soft tissues is significantly different, separating between a healthy and a frail residuum.

The purpose of this study is therefore to apply patient-specific magnetic resonance imaging (MRI) based non-linear finite element (FE) models to quantify the internal mechanical states in multiple residual limbs of TTA prosthetic users during load-bearing.

O. Dössel and W.C. Schlegel (Eds.): WC 2009, IFMBE Proceedings 25/IX, pp. 28–31, 2009.
www.springerlink.com

II. METHODS

In a recent study [2] we introduced a patient-specific FE three-dimensional (3D) modeling technique of the TTA residuum using MRI. The FE model was used to quantify internal strains and stresses in the confined residual limb during load-bearing. In order to obtain the geometry of the bones, muscle and fat tissues during upright standing position, the TTA patient donned a plaster cast, prepared before the trial and stood inside an open-MRI ("Signa SP'' model, General Electric Co., CT, USA). Two scans were performed: the first taken while no pressure was applied to the residuum and the second scan was taken while the patient applied partial body weight to the residuum, against the MRI table. During the second trial we used thin force sensors (FlexiForce, Tekscan Co. MA, USA) to verify load bearing in this posture.

Three traumatic unilateral TTA patients participated so far in our ongoing research. All the patients chosen for this study are active individuals, who use their prosthesis for several hours on a daily basis. Helsinki approval (#4302/06 from Sheba Medical Center, Ramat-Gan, Israel) and informed consents were obtained before the trials. Table 1 lists patient information for the participating subjects.

Table 1 Patient information for the participants

Patient #	#1	#2	#3
Gender	Female	Male	Male
Age (years)	32	44	63
Amputated limb	Right	Left	Right
Weight (kg)	50	82	64
Years post-amputation	2	4	41
Illnesses	-	Diabetes	-

The transversal MRI scans of the unloaded residuum were uploaded to a solid modeling software (SolidWorks 2009, SolidWorks, MA, USA). Then, a 3D solid model of the truncated bones, muscle flap, fat and plaster cast was exported to an FE modeling software (ABAQUS v. 6.8, SIMULIA, RI, USA) for non-linear large deformation analyses. A 2mm skin layer was configured in the FE software. We measured the downward displacement of the tibia and fibula, relative to the most distal point of the limb at the scans with and without load-bearing. This displacement was used as a boundary condition applied to the FE bones. The exterior surface of the plaster cast was constrained for all translations. A friction coefficient of 0.7 was set between the skin and the cast. All the internal surfaces, i.e. fat/muscle and muscle/bones, were tied together.

By imposing the downward displacements of the bones, measured in the MRI trials for each patient, we were able to calculate 3D distributions of soft tissue strains per each model. Since the patient-specific mechanical properties of the muscle, fat and skin tissues of the individuals were unknown, we refrained from further calculating stresses from the strain tensors. However, since ABAQUS formally requires definitions of constitutive laws and properties for each model component, these were defined as follows. The bones were assumed to be rigid. The cast was assumed to be a homogeneous, isotropic and linear-elastic material, with elastic modulus of 1GPa and Poisson's ratio of 0.3. All the soft tissues were assumed to be hyperelastic, homogeneous and isotropic, and were modeled using the Generalized Mooney-Rivlin Solid strain energy function [3]:

$$W = C_{10}(I_1 - 3) + C_{11}(I_1 - 3)(I_2 - 3) + \frac{1}{D_1}(J-1)^2 \quad (1)$$

where the invariants of the principal stretch ratios λ_i are $I_1 = \lambda_1^2 + \lambda_2^2 + \lambda_3^2$ and $I_2 = \lambda_1^{-2} + \lambda_2^{-2} + \lambda_3^{-2}$, the relative volume change is $J = \lambda_1\lambda_2\lambda_3$, and C_{10}, C_{11}, D_1 are the constitutive parameters. Values for the constitutive parameters C_{10}, C_{11}, D_1 were adopted from the literature for all soft tissues, and are specified in Table 2.

Table 2 Material parameters for soft tissues of the transtibial residuum represented using eq. (1)

Soft tissue	C_{10} [kPa]	C_{11} [kPa]	D_1 $\left[MPa^{-1}\right]$
Fat	0.143	0	70.2
Muscle	4.25	0	2.36
Skin	9.4	82	0

The bones were meshed with 4-node quadrilateral surface elements ("SFM3D4" in ABAQUS). The muscle flap, fat tissue and plaster cast were meshed with second-order 10-node modified quadratic tetrahedron elements ("C3D10M"). The skin tissue was meshed with 6-node quadratic triangular membrane elements (''M3D6'').

We calculated distributions of principal compression and tension strains, maximal shear strain and strain energy density (SED). Strains are reported here as engineering strains. We defined two separate muscular volumes of interests (VOI; Fig 1b): The first VOI is a layer of all the elements contacting the third distal end of the tibia, i.e. the bone proximity layer (BPL) and a second VOI of all the elements contacting the fat/skin tissues, that are under the projection of the distal third of the tibia, and that are located not higher than the height of the distal third of the tibia, i.e. fat proximity layer (FPL).

III. RESULTS

The geometrical characteristics of the transtibial residual limbs measured on the 3D patient-specific solid model are specified in Table 3. According to our measurements, patient #2 had the longest residuum, manifesting in longer tibia and fibula. Additionally, the soft tissue bulk of patient #2 was thicker as the muscle cushioning the distal tibial end

was 2.5-fold and 10-fold thicker than the flap muscle under the tibias of patients #3 and #1, respectively (Table 3). The volume of the muscle flap of patient #2 was more than 3-fold greater than the volumes of the muscle flap of patients #1 and #3. Patient #1 is very thin so that no fat tissue could be isolated from her MRI scans for the solid model. The limb of patient #3 was amputated at the most proximal location compared to patients #1 and #2, resulting in the shortest tibial length (Table 3). The residuum of patient #3 had a conical shape as opposed to the more cylindrical shapes of the residuum of patients #1 and 2.

Table 3 Geometrical characteristic of the residual limbs

Patient #		#1	#2	#3
Length [cm]	Tibia	9	11.2	6.8
	Fibula	5.1	8.9	5.3
	Muscle flap under the tibia	0.2	2.1	0.8
Bevelment [°]	Tibia	12.5	52.3	18
Cross-sectional area [cm^2]	At the tibial tuberosity	10	14.9	14.5
	Central tibia	5.8	8.1	10.5
	Distal tibia	1.3	1.5	2.1
	Central fibula	0.65	0.6	0.64
	Distal fibula	0.3	0.2	0.1
	Central muscle	39.2	58.8	43.8
	Distal muscle	9.2	33.6	5.0
Volume [cm^3]	Muscle	196.3	702	183.3
	Fat	0	90.2	13.7
	Skin	38.1	92.4	39.6

Vertical displacements of 1, 1.6 and 1.8mm of the bones towards the MRI table were measured on the loaded and unloaded coronal MRI scans of patient #1 to #3, respectively. The mean principal compression and tension strains, maximal shear strain and SED are presented in Table 4 for the three TTA patients. Generally, mean internal strains at the tibial proximity were higher than mean strains at muscle tissue near the skin of the residuum. Mean strains found in the residual limb of patient #2 were one magnitude of order lower than mean strains found in the residual limbs of patients #1 and 3.

Table 4 Mean principal compression and tension strain, maximal shear strain and SED for the three TTA patients. Values in parentheses are standard deviations from the mean.

Patient #		#1	#2	#3
Mean principal compressive strain [%]	BPL	12.8 (9.7)	3.1 (1.3)	14.2 (9.1)
	FPL	6.2 (8.8)	2.5 (1.1)	13.7 (11.8)
Mean principal tensile strain [%]	BPL	11.1 (7.1)	2.8 (1.4)	12.6 (7.7)
	FPL	5.0 (7.0)	2.0 (0.7)	11.1 (10.2)
Mean maximal shear strain [%]	BPL	12.6 (9.9)	2.9 (1.3)	14.9 (10.4)
	FPL	6.1 (9.1)	2.5 (0.8)	13.1 (11.4)
Mean strain energy density [kJ/m^3]	BPL	734 (1844)	47.4 (43.4)	734 (1228)
	FPL	370 (1483)	14.8 (12.2)	863 (1168)

Figure 1 depicts the principal compression and tension strains, maximal shear strain and SED in the flap muscle of the three TTA patients in a sagittal view through the tibia. Since the fat tissue of patient #3 was embedded in the muscle tissue, it is included in the representation of strains in Figure 1.

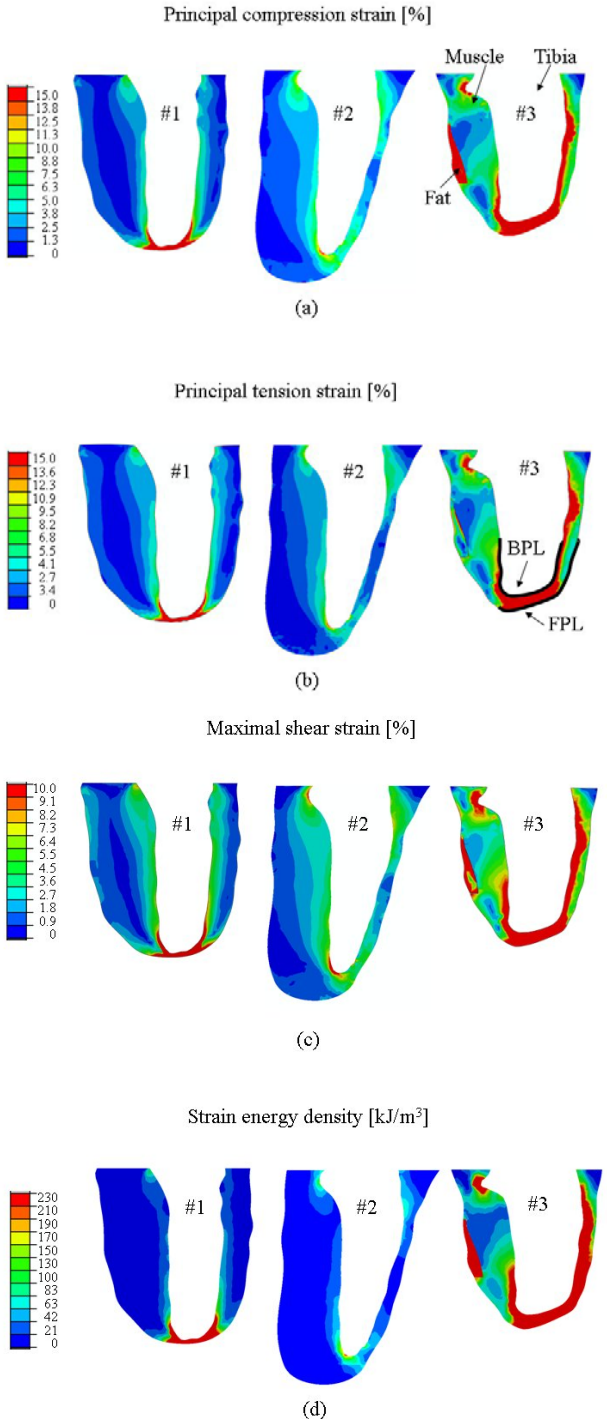

Fig. 1 The (a) principal compression [%] and (b) tension strain [%], (c) maximal shear strain [%] and (d) strain energy density [kJ/m^3] in the muscle tissues of the three transtibial amputation patients.

The percentage of volume of the muscle tissue at the BPL and FPL that holds principal compression strains above 5% (i.e. large strains) are presented in Fig 2. These results clearly show low compression strains in the longer residuum of patient #2 and higher compression strains in the shorter residual limbs of patients #1 and 3.

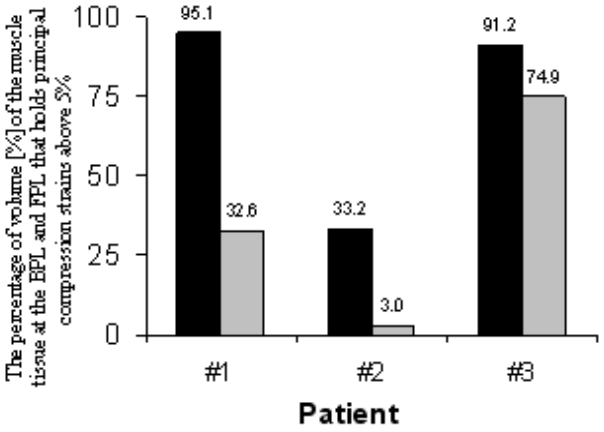

Fig. 2 The percentage of volume [%] of the muscle tissue at the BPL and FPL that holds principal compression strains above 5%

IV. CONCLUSIONS

In this study, we used patient-specific 3D FE modeling of the residual limbs of TTA patients during standing in an open MRI setting while applying body weight to their residual limb. We found high strains in the BPL rather than in the FPL (Table 4; Figs 1,2). This finding alerts to the susceptibility of the TTA muscle flap to DTI in the proximity of the distal end of the tibia.

The highest strains were found in the shortest residuum of patient #3. This is partially because the vertical movement of the bones found on the MRI scans of this patient was the greatest between the three patients. Correspondingly, the lowest strains were found in the longest residuum with the thickest muscle flap. Yet even in the case of a long residuum, a third of the distal tibial proximity area was occupied by internal principal compression strains above 5%. For the two TTA patients with shorter residual limbs, the internal principal compression strains above 5% occupied almost the entire distal tibial proximity area.

We conclude that the wide viability between TTA residual limbs necessitate quantitative analysis of the internal mechanical state in the TTA individual to assess the risk for DTI onset.

REFERENCES

1. Agam L, Gefen A (2007) Pressure ulcers and deep tissue injury: a bioengineering perspective. J Wound Care 16:336-342.
2. Portnoy S, Yizhar Z, Shabshin N, Itzchak Y, Kristal A, Dotan-Marom Y, Siev-Ner I, Gefen A (2008) Internal mechanical conditions in the soft tissues of a residual limb of a trans-tibial amputee. J Biomech 41:1897-1909.
3. Mooney MA (1940) Theory of large elastic deformation. J Appl Phys 11:582-592.

Author: Prof. Amit Gefen
Institute: Tel Aviv University
Street: Klauzner
City: Ramat Aviv
Country: Israel
Email: gefen@eng.tau.ac.il